Tunneling Anisotropic Magnetoresistance at the Single-Atom Limit

N. Néel,[1,*] S. Schröder,[2,†] N. Ruppelt,[1] P. Ferriani,[2] J. Kröger,[3] R. Berndt,[1] and S. Heinze[2]

[1]*Institut für Experimentelle und Angewandte Physik, Christian-Albrechts-Universität zu Kiel, D-24098 Kiel, Germany*
[2]*Institut für Theoretische Physik und Astrophysik, Christian-Albrechts-Universität zu Kiel, D-24098 Kiel, Germany*
[3]*Institut für Physik, Technische Universität Ilmenau, D-98693 Ilmenau, Germany*

(Received 17 October 2012; revised manuscript received 19 December 2012; published 18 January 2013)

The tunneling anisotropic magnetoresistance (TAMR) of single Co atoms adsorbed on a double-layer Fe film on W(110) is observed by scanning tunneling spectroscopy. Without applying an external magnetic field the TAMR is found by comparing spectra of atoms that are adsorbed on the domains and domain walls of the Fe film. The TAMR can be as large as 12% and repeatedly changes sign as a function of bias voltage. First-principles calculations show that the hybridization between Co d states of different orbital symmetries depends on the magnetization direction via spin-orbit coupling. This leads to an anisotropy of the density of states and thus induces a TAMR.

DOI: 10.1103/PhysRevLett.110.037202 PACS numbers: 75.47.−m, 68.37.Ef, 73.40.Gk, 75.70.Tj

The resistance of a tunneling junction involving a single ferromagnetic layer may depend on the magnetization direction relative to the crystallographic axes. This effect has first been observed in scanning tunneling microscopy experiments [1]. It was also reported in planar tunnel junctions with ferromagnetic semiconductors and coined tunneling anisotropic magnetoresistance (TAMR) [2]. It is caused by spin-orbit coupling, which results in an anisotropy of the density of states [1–4]. The TAMR is attractive for spintronics applications as it requires only one magnetic layer and does not rely on coherent spin-dependent transport [2]. The effect has also been predicted to occur for magnetic transition-metal electrodes, which exhibit significantly higher Curie temperatures [5,6]. Related experiments have been reported from Fe/GaAs/Au junctions [7] as well as from CoFe films separated by oxide layers [8]. The TAMR, typically defined as the difference of the conductances for the two magnetization directions divided by the conductance in one of the configurations, can be enhanced by two orders of magnitude up to some 10% by combining $3d$- and $5d$-transition metals [9]. Junctions with antiferromagnetic electrodes may be another route toward room-temperature applications [10,11].

Presently, little is known about how the TAMR scales down to the nanometer scale and, ultimately, to the single atom limit. Theoretical studies have predicted rapid oscillations of the TAMR with bias voltage and giant values of up to 200% in atomic-scale contacts due to tip resonance states [12]. Conclusive experimental investigations into the magnetoresistance of atomic junctions, however, are challenging. Nanoscale contacts fabricated by the mechanically controllable break junction technique were reported to give giant TAMR values of up to 100% [13]. For contacts formed by electromigration, a TAMR of 25% and bias-voltage-dependent changes on the scale of a few mV have been observed [14]. However, a comparison with theory is difficult because the microscopic structure of such junctions is unknown [12–14]. Another obstacle to an unambiguous interpretation of these data is the use of an external magnetic field, which may deform the contacts via magnetostatic or magnetostrictive forces. Scanning tunneling microscopy (STM) with nonmagnetic tips opens the possibility of circumventing these problems. Magnetic domain walls [1] and even noncollinear magnetic structures [15,16] have been imaged exploiting the TAMR. It has further been proposed from theory to detect the spin direction of a single Mn dopant atom in GaAs using STM [17].

Here, we report scanning tunneling spectroscopy measurements of the bias-voltage-dependent TAMR of single Co atoms adsorbed on a double-layer Fe film on W(110). The Fe double layer on W(110) displays domains with an out-of-plane magnetization direction that rotates into the film plane within the domain walls. Because Co adatoms couple ferromagnetically to the Fe double layer, their magnetic moment is oriented parallel to the local magnetization of the Fe film. Tunneling spectra from Co adatoms on domains and domain walls therefore probe the TAMR without the need of an external magnetic field. Oscillations of the TAMR in a bias-voltage range of 100 mV and absolute values of up to 12% were observed. These experimental findings are explained based on density functional theory (DFT) calculations. It is demonstrated that the hybridization between Co d states of different orbital symmetries depends on the magnetization direction via spin-orbit coupling. This leads to an anisotropy of the density of states and thus induces a TAMR.

The experiments were performed with a homemade scanning tunneling microscope operated at 7 K and in ultrahigh vacuum with a base pressure of 10^{-9} Pa. W(110) surfaces were cleaned by oxidation cycles at 1400 K and brief annealing at 2200 K. Room-temperature exposure of clean W(110) to an Fe atom flux from an electron beam evaporator and subsequent annealing at 500 K results in a closed Fe film on top of a Fe wetting

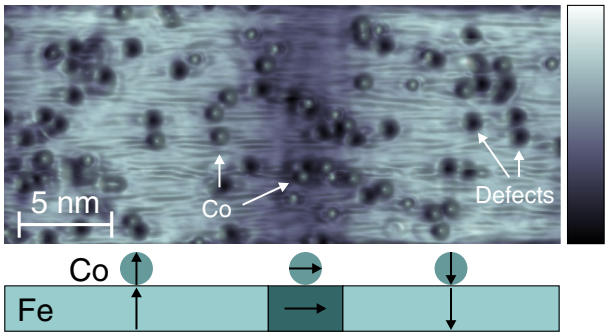

FIG. 1 (color online). Pseudo-three-dimensional representation of a constant-current STM image (1 nA, 0.07 V) of Co atoms adsorbed on a double-layer Fe film on W(110). To visualize the magnetic domains and domain walls, the topography data have been colored with the simultaneously recorded dI/dV map. The color scale ranges from 5 (dark) to 14 nS (bright). The sketch at the bottom of the figure shows the alignment of the Co magnetic moment with the Fe magnetization.

layer [18]. Single Co atoms were deposited onto Fe-covered W(110) at 10 K. Figure 1 shows that Co atoms adsorb to magnetic domains and domain walls, which are imaged with high and low contrast, respectively. The contrast is due to different magnetization directions, whose signature is imprinted on the probed electronic structure via the spin-orbit interaction [1]. Magnetic domains exhibit an out-of-plane ($\perp$) magnetization while the central regions of domain walls are in-plane ($\parallel$) magnetized along [001] [19]. W tips were fabricated from polycrystalline wire, which was chemically etched and annealed *in vacuo* prior to mounting. An eventual spin polarization of the tip was reduced by single-atom transfers from the tip to the surface [20]. To determine the spin-polarization spectra and maps of the differential conductance (dI/dV) were acquired from double-layer Fe islands, which in the case of a spin-polarized tunneling current give rise to clear spin contrast [1]. Spectroscopy was performed by modulating the bias voltage (1 mV_{rms}, 8 kHz) and measuring the current response with a lock-in amplifier.

The dI/dV spectra shown in Fig. 2(a) were obtained with a W tip from Co atoms adsorbed either on the domains (dashed red line) or on the domain walls (solid blue line) of the Fe film. Owing to the strong exchange coupling between Co and Fe the magnetic moment of Co adatoms is oriented out-of-plane and in-plane on domains and domain walls, respectively [21]. The two spectra are similar. To emphasize the differences, Fig. 2(b) shows the TAMR defined as

$$\mathrm{TAMR} = \frac{dI_\perp/dV - dI_\parallel/dV}{dI_\perp/dV}, \qquad (1)$$

where $I_\perp$ ($I_\parallel$) denotes the tunneling current across a Co atom adsorbed on a magnetic domain (domain wall) of the Fe double layer. Obviously, the sign of the TAMR

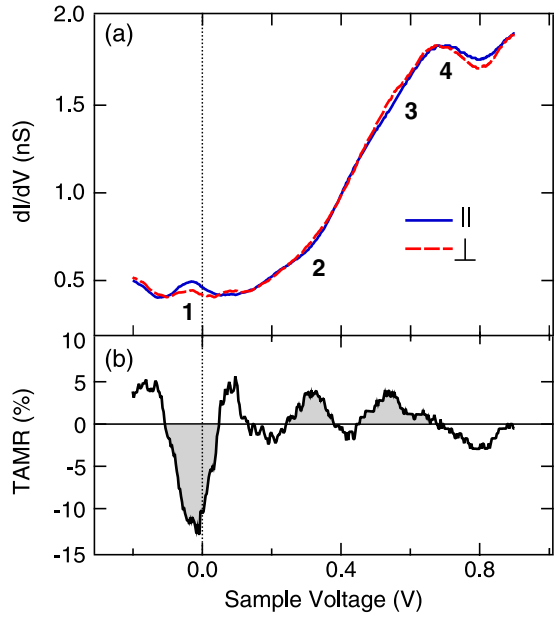

FIG. 2 (color online). (a) dI/dV spectra obtained on Co adatoms on domains (red dashed line) and on domain walls (blue solid line) of an Fe double-layer film on W(110). The feedback loop had been disabled at 0.9 V and 1 nA prior to spectroscopy. To facilitate comparison with calculations (Fig. 3) some spectroscopic features are labeled 1–4. (b) Tunneling anisotropic magnetoresistance determined from the spectra in (a). The TAMR at the features 1 to 4 are shaded for easier comparison with Fig. 3.

repeatedly changes sign. A maximum magnitude of 12% is reached close to zero voltage.

To explain the TAMR of the Co adatoms we performed DFT calculations applying the full-potential linearized augmented plane-wave method [22] as implemented in the FLEUR code [23]. A symmetric film as described in Refs. [21,24] was used. While structural relaxations were carried out within the generalized gradient approximation [25], the electronic structure was analyzed within the local density approximation [26]. Spin-orbit coupling was included by means of a second variational approach [27]. $12\mathbf{k}_\parallel$ points in the irreducible wedge of the two-dimensional Brillouin zone and a plane-wave cutoff of $k_{max} = 3.9$ a.u^{-1} were used. The local density of states (LDOS) was calculated using $468\mathbf{k}_\parallel$ points in the entire Brillouin zone.

We compare the experimental dI/dV spectra with the calculated LDOS in the vacuum. Figure 3(a) shows the calculated vacuum LDOS above the Co adatom for $\perp$ (dashed red) and $\parallel$ magnetizations (solid blue line) along the [001] direction [19]. Four peaks 1 to 4 may be distinguished in the LDOS at energies of -0.07, 0.16, 0.56, and 0.78 eV, respectively, relative to the Fermi level. These peaks can be identified with those obtained in the experimental dI/dV spectra [Fig. 2(a)] at voltages of -0.02, 0.32, 0.52, and 0.7 V [28].

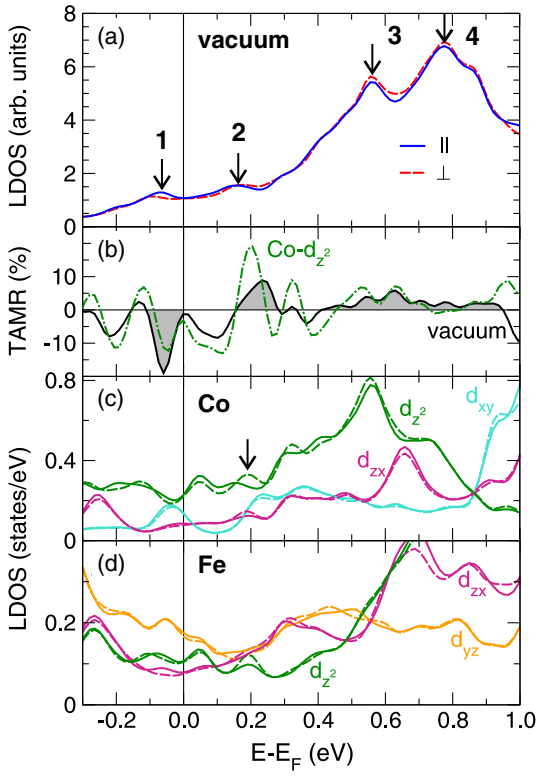

FIG. 3 (color online). (a) Vacuum local density of states in arbitrary units at a tip-sample distance $z = 0.6$ nm above a Co adatom on an Fe double layer on W(110) calculated for a spin-quantization axis aligned parallel ($\parallel$, solid blue line) and perpendicular ($\perp$, dashed red line) to the film plane. Peaks exhibiting a difference between the vacuum LDOS for $\parallel$ and $\perp$ magnetizations are indicated by arrows. (b) TAMR of the vacuum LDOS (solid black line) shown in (a) and of the minority spin d_{z^2} LDOS of the Co adatom (dashed-dotted green line) shown in (c). (c),(d) Orbital symmetry decomposition of the minority spin LDOS (in the muffin tin) of the Co adatom and the adjacent Fe atom, respectively, with $\parallel$ (solid lines) and $\perp$ (dashed lines) spin-quantization axes.

The vacuum LDOS of the different magnetization directions exhibits small deviations due to spin-orbit coupling (SOC). This leads to bias-dependent oscillations of the TAMR, which is calculated from the anisotropy of the LDOS, namely $(\mathrm{LDOS}_\perp - \mathrm{LDOS}_\parallel)/\mathrm{LDOS}_\perp$ [Fig. 3(b)]. For clarity the TAMR at the LDOS features 1 to 4 of Fig. 3(a) have been shaded. Peaks 2 to 4 show an enhanced vacuum LDOS above $\perp$ magnetized Co, i.e., a positive sign of the TAMR, in agreement with the experimental data of Fig. 2. The vacuum LDOS of peak 1 on the other hand is larger above $\parallel$ magnetized Co, which results in a negative TAMR as observed in the experiments. The calculated TAMR values range from approximately -19% to 9% in reasonable agreement with the experimental values ranging between -12% to 5%. The overall oscillatory evolution of the calculated TAMR with energy is in good agreement with the voltage dependence of the experimental TAMR.

To understand the origin of the TAMR, the LDOS of the Co adatom was decomposed according to orbital symmetries [Fig. 3(c)]. The changes due to SOC stem from the $3d$ states of Co, which possess a low LDOS around the Fermi energy for the majority spin channel. Therefore, we focus on the minority states below. A comparison of the vacuum [Fig. 3(a)] and the minority spin [Fig. 3(c)] LDOS of a Co atom reveals that the peaks 2–4 originate from states of d_{z^2} character. The small feature below the Fermi energy 1 can be attributed to a hybridized state between the Co adatom and the Fe film. It is of d_{xy} type at the Co adatom, Fig. 3(c), and of d_{yz} character in the Fe film, Fig. 3(d).

The change of the vacuum LDOS for $\parallel$ and $\perp$ magnetizations is also observed in the orbitally decomposed LDOS at the Co adatom. In particular, the solid and dashed curves for the d_{z^2} states display the same differences as the vacuum LDOS at the peaks 1 to 4 [cf. also the TAMR from the d_{z^2} states shown in Fig. 3(b)]. These changes can be understood based on mixing of the d_{z^2} states with d states of different orbital symmetry via spin-orbit coupling. This is most easily seen for peak 2. Being mainly of d_{z^2} character at the Co adatom, it is shifted to higher energies and enhanced at $\perp$ magnetization with respect to the in-plane d_{z^2} density of states [Fig. 3(c)]. There is also a small enhancement of the $\mathrm{LDOS}_\perp$ of the d_{zx} orbitals at the same energy, which indicates a hybridization of the d_{zx} and d_{z^2} orbitals.

The essential physics of the LDOS anisotropy can be captured in a simple model of two interacting, localized atomic states at a surface:

$$\left[E \cdot \mathbb{1} - \begin{pmatrix} \varepsilon_1 & -t \\ -t & \varepsilon_2 \end{pmatrix} - \begin{pmatrix} i\gamma_1 & 0 \\ 0 & i\gamma_2 \end{pmatrix}\right] G(E) = \mathbb{1}. \quad (2)$$

Here $\varepsilon_{1,2}$ are the energies of the two states, t is the hopping between them which depends on the magnetization direction via spin-orbit coupling, and the diagonal elements $i\gamma_{1,2}$ simulate the hybridization with the substrate, which broadens the peaks. The Green function $G(E)$ is a 2×2 matrix and the LDOS of state i, $D_i(E)$, is obtained from the diagonal elements of the Green function by $D_i(E) = -\pi^{-1}\mathrm{Im}G_{ii}(E)$. We choose the energy difference and the energy broadening of the two states according to the d_{z^2} and the d_{zx} peaks at $+0.19$ eV in the Co adatom LDOS, Fig. 3(c). The coupling of the two states due to SOC is governed by the Hamiltonian $H_{\mathrm{SOC}} = \xi \mathbf{ls}$ with spin, $\mathbf{s}$, and angular momentum, $\mathbf{l}$, operators. The SOC constant ξ is on the order of 40 meV for $3d$-transition metals [29]. The matrix element for the mixing between minority spin states, $\downarrow$, of d_{zx} and a d_{z^2} orbital character, $t = \langle \downarrow, d_{zx}|H_{\mathrm{SOC}}|\downarrow, d_{z^2}\rangle$ [30], vanishes for perpendicular magnetization whereas it is maximal for parallel magnetization. Therefore, we use $t = 0$ and $t = 40$ meV for the $\perp$ and $\parallel$ magnetization directions, respectively.

Figure 4(a) shows the LDOS obtained from the model for the two peaks and the two magnetization directions. The LDOS at both peak positions is larger for a $\perp$ magnetization

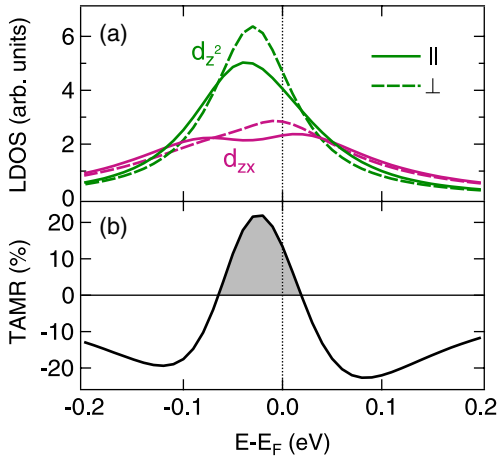

FIG. 4 (color online). LDOS obtained for a model of two atomic states at a surface, which are of different orbital symmetry and couple via SOC. (a) A d_{z^2} and a d_{zx} state for ∥ (solid line) and ⊥ (dashed) magnetizations. (b) LDOS anisotropy (TAMR) of the d_{z^2} state as defined in the text.

[Fig. 4(a)] in agreement with the DFT calculation [cf. Fig. 3(c)]. We obtain the TAMR within this model, Fig. 4(b), by considering only the LDOS of the d_{z^2} state, which provides the major contribution to the vacuum LDOS. The model yields a TAMR with a shape similar to that of a single peak in Fig. 3(b) with a maximum close to the LDOS peak positions and a change of sign at both higher and lower energies. As the simple model does not take into account that the state also comprises some s and p_z character that contribute to the vacuum LDOS, the TAMR is increased in the model with respect to the DFT calculation.

In conclusion, TAMR was observed from single Co atoms adsorbed on a double layer of Fe on W(110) using STM. The TAMR shows rapid sign reversals with bias voltage. Its absolute values are on the order of 10%, which is drastically lower than theoretically predicted values for perfectly symmetric junctions [12]. DFT calculations demonstrate that the TAMR is due to mixing of Co d resonances with different orbital characters that depend on the magnetization direction due to SOC. Using our experimental approach it is possible to explore the TAMR at the atomic scale without external magnetic fields, which will allow future systematic studies for different atom types or atomic-scale structures.

Funding of the DFG via SFB 668 and project HE3292/8-1 is acknowledged. We thank Gustav Bihlmayer for insightful discussions and the HRLN for providing computational time.

*Present address: Institut für Physik, Technische Universität Ilmenau, D-98693 Ilmenau, Germany.
†Corresponding author.
schroeder@theo-physik.uni-kiel.de

[1] M. Bode, S. Heinze, A. Kubetzka, O. Pietzsch, X. Nie, G. Bihlmayer, S. Blügel, and R. Wiesendanger, Phys. Rev. Lett. **89**, 237205 (2002).
[2] C. Gould, C. Rüster, T. Jungwirth, E. Girgis, G. M. Schott, R. Giraud, K. Brunner, G. Schmidt, and L. W. Molenkamp, Phys. Rev. Lett. **93**, 117203 (2004).
[3] A. Matos-Abiague and J. Fabian, Phys. Rev. B **79**, 155303 (2009).
[4] A. Matos-Abiague, M. Gmitra, and J. Fabian, Phys. Rev. B **80**, 045312 (2009).
[5] A. B. Shick, F. Maca, J. Masek, and T. Jungwirth, Phys. Rev. B **73**, 024418 (2006).
[6] A. N. Chantis, K. D. Belashchenko, E. Y. Tsymbal, and M. van Schilfgaarde, Phys. Rev. Lett. **98**, 046601 (2007).
[7] J. Moser, A. Matos-Abiague, D. Schuh, W. Wegscheider, J. Fabian, and D. Weiss, Phys. Rev. Lett. **99**, 056601 (2007).
[8] L. Gao, X. Jiang, S.-H. Yang, J. D. Burton, E. Y. Tsymbal, and S. S. P. Parkin, Phys. Rev. Lett. **99**, 226602 (2007).
[9] B. G. Park, J. Wunderlich, D. A. Williams, S. J. Joo, K. Y. Jung, K. H. Shin, K. Olejník, A. B. Shick, and T. Jungwirth, Phys. Rev. Lett. **100**, 087204 (2008).
[10] A. B. Shick, S. Khmelevskyi, O. N. Mryasov, J. Wunderlich, and T. Jungwirth, Phys. Rev. B **81**, 212409 (2010).
[11] B. G. Park, J. Wunderlich, X. Marti, V. Holý, Y. Kurosaki, M. Yamada, H. Yamamoto, A. Nishide, J. Hayakawa, H. Takahashi *et al.*, Nat. Mater. **10**, 347 (2011).
[12] J. D. Burton, R. F. Sabirianov, J. P. Velev, O. N. Mryasov, and E. Y. Tsymbal, Phys. Rev. B **76**, 144430 (2007).
[13] M. Viret, M. Gabureac, F. Ott, C. Fermon, C. Barreteau, G. Autes, and R. Guirado-Lopez, Eur. Phys. J. B **51**, 1 (2006).
[14] K. I. Bolotin, F. Kuemmeth, and D. C. Ralph, Phys. Rev. Lett. **97**, 127202 (2006).
[15] S. Heinze, K. von Bergmann, M. Menzel, J. Brede, A. Kubetzka, R. Wiesendanger, G. Bihlmayer, and S. Blügel, Nat. Phys. **7**, 713 (2011).
[16] K. von Bergmann, M. Menzel, D. Serrate, Y. Yoshida, S. Schröder, P. Ferriani, A. Kubetzka, R. Wiesendanger, and S. Heinze, Phys. Rev. B **86**, 134422 (2012).
[17] J.-M. Tang and M. E. Flatté, Phys. Rev. B **72**, 161315(R) (2005).
[18] A. Kubetzka, M. Bode, O. Pietzsch, and R. Wiesendanger, Phys. Rev. Lett. **88**, 057201 (2002).
[19] M. Heide, G. Bihlmayer, and S. Blügel, Phys. Rev. B **78**, 140403 (2008).
[20] M. Ziegler, N. Ruppelt, N. Néel, J. Kröger, and R. Berndt, Appl. Phys. Lett. **96**, 132505 (2010).
[21] M. Ziegler, N. Néel, C. Lazo, P. Ferriani, S. Heinze, J. Kröger, and R. Berndt, New J. Phys. **13**, 085011 (2011).
[22] E. Wimmer, H. Krakauer, M. Weinert, and A. J. Freeman, Phys. Rev. B **24**, 864 (1981).
[23] http://www.flapw.de.
[24] N. Néel, P. Ferriani, M. Ziegler, S. Heinze, J. Kröger, and R. Berndt, Phys. Rev. B **85**, 155406 (2012).
[25] Y. Zhang and W. Yang, Phys. Rev. Lett. **80**, 890 (1998).
[26] S. H. Vosko, L. Wilk, and M. Nusair, Can. J. Phys. **58**, 1200 (1980).

[27] H. J. F. Jansen and A. J. Freeman, Phys. Rev. B **30**, 561 (1984).
[28] We attribute the small deviations between the experimental and theoretical peaks to the fact that the exchange-correlation functional is only an approximation to the self-energy. Note that there may be a self-interaction error to the peak positions that depends on the localization of a given state.
[29] P. Bruno, Phys. Rev. B **39**, 865 (1989).
[30] E. Abate and M. Asdente, Phys. Rev. **140**, A1303 (1965).